chemengineering

MDPI

Article

Insights from Mathematical Modelling into Process Control of Oxygen Transfer in Batch Stirred Tank Bioreactors for Reducing Energy Requirement

John J. Fitzpatrick *, Franck Gloanec and Elisa Michel

Process & Chemical Engineering, School of Engineering, University College Cork, T12 K8AF Cork, Ireland; franck.gloanec@ensiacet.fr (F.G.); elisa_michel@aol.fr (E.M.)

* Correspondence: j.fitzpatrick@ucc.ie; Tel.: +353-21-4903-089

Received: 14 April 2020; Accepted: 25 May 2020; Published: 26 May 2020

Abstract: Significant energy savings can be made in aerobic stirred tank batch bioreactors by the manipulation of agitator power (*Pag*) and air flowrate per unit working volume (*vvm*). Control is often implemented to maintain the oxygen concentration in the bioreaction liquid (C_{OL}) at a constant value. This work used model simulations to show that controlling the *Pag* and *vvm* continuously over time, such that it is operated at or near the impeller flooding constraint results in the minimum energy requirement for oxygen transfer (strategy Cmin); however, this might prove impractical to control and operate in practice. As an alternative, the work shows that dividing the bioreaction time into a small number of constant *Pag* time segments (5–10), where a PID controller is used to control *vvm* to maintain C_{OL} constant in each segment, can achieve much of the energy saving that is associated with Cmin. During each time segment, *vvm* is increased and a sudden decrease in C_{OL} is used to detect the onset of flooding, after which there is a step increase in *Pag*. This sequence of *Pag* step increases continues until the bioreaction is completed. This practical control approach was shown to save most of the energy that is associated with Cmin.

Keywords: process control; energy efficiency; oxygen transfer; batch stirred tank bioreactor; mathematical modelling

1. Introduction

In aerobic bioreactors, oxygen is critical for microbial activity and it can easily become rate limiting, thus continuous supply is required [1]. In aerobic batch stirred tank bioreactors, the oxygen uptake rate (*OUR*) of the micro-organisms will vary over the batch bioreaction time and an aeration system is required to supply a sufficient oxygen transfer rate (*OTR*) to satisfy the *OUR* of the micro-organisms. This typically consists of an air compressor to provide air that enters as bubbles and a mechanical agitator that greatly improves the oxygen transfer rate (*OTR*). Many studies have shown how agitation and air flowrate influence *OTR* and, in turn, influence cell growth and the production of metabolites [2–9].

For stirred tank aerobic bioreactors, the aeration system is energy intensive with energy being required for the air compressor and mechanical agitator. This represents a significant cost in aerobic bioreactors [10] and contributes to the environmental impact that is associated with the consequential carbon footprint of the bioreactors. When considering this, it is becoming increasingly important to reduce cost [11] and carbon footprint by using energy more efficiently. Proper equipment selection, such as the selection of impeller type and impeller dimensions [12–14], can reduce aeration system energy and associated costs and carbon footprint. Hydrodynamics will strongly influence the rate of oxygen mass transfer [15–18] in a given stirred bioreactor. The agitator mechanical power input (*Pag*) and air volumetric flowrate (F_G) are under direct operational control and can be manipulated

to produce a volumetric mass transfer coefficient (k_La) that can provide sufficient *OTR* to meet the *OUR*. Reducing aeration system energy requirement can be achieved by optimal operation of *Pag* and F_G [12,19–21].

Process control can improve the performance of bioreactors [22–26]. The control of *Pag* and F_G is used to control the oxygen transfer rate in aerobic bioreactors. A commonly used practical control strategy is to measure the oxygen concentration in the bioreaction liquid and use this information to vary F_G and/or *Pag* throughout the bioreaction, so as to maintain the oxygen concentration close to a constant value. Many combinations of the two can potentially deliver the same *OTR* that satisfies the *OUR* required in order to maintain a constant oxygen concentration [20]. When the total agitator and compressor energies are summed over the duration of the bioreaction, the total energy requirement that is associated with each combination will vary. Consequently, this presents an opportunity to reduce energy by manipulating and controlling *Pag* and/or F_G throughout the bioreaction to provide an *OTR* that satisfies the *OUR* requirement while using less total energy [19,20,27]. Furthermore, it represents an opportunity to minimise total energy by determining the combinations of *Pag* and F_G over the bioreaction time that minimises the total energy requirement.

Some studies have shown that operating at or close to the onset of flooding throughout the bioreaction can minimise the total energy requirement. Kreyenschulte et al. [28] developed a computation tool for assessing aeration system energy demand at the large-scale. For bioreactor volumes of 20 m^3 and larger using conventional agitators, they showed that the minimum energy consumption was achieved by operating close to the onset of flooding. Fitzpatrick et al. [29] performed a mathematical modelling study, which showed that energy was minimised by operating at or close to the onset of flooding. Of course, this approach to energy reduction might be limited by other constraints, such as foaming and use of antifoams, the production of carbon dioxide, and damage to cells [18,30]. The shear sensitivity of mammalian cells will influence the selection of air spargers and impellers, and will limit air flowrates and the specific power input of agitators [18].

This work focusses on bioreactor process control to achieve energy reduction/minimisation for oxygen transfer in a batch stirred tank aerobic bioreactor. A bioreaction model is used to simulate a bioreaction and the only output variable that is used by the process controller is the oxygen concentration in the bioreaction liquid. The objective is to investigate the application of PID process control to manipulating F_G and/or *Pag*, so that the energy for oxygen transfer is reduced or minimised, while also maintaining the oxygen concentration at a constant value.

2. Mathematical Modelling and Aeration System Control Strategies

2.1. Mathematical Modelling

The bioreactor simulated in this study had a working volume of 20 m^3. A six bladed Rushton turbine impeller was used with a standard design configuration. The mathematical models, along with relevant parameter values, used for bioreaction kinetics, *OUR*, *OTR*, agitator, and compressor power requirements, phase equilibrium, and flooding constraints have already been presented in this journal by Fitzpatrick et al. [29], based on previous work that was conducted by the group.

2.2. Aeration System Control Strategies

A commonly used practical control strategy is to maintain the oxygen concentration in the bioreaction liquid (C_{OL}) at a constant value, by controlling F_G (or *vvm*) and/or *Pag* throughout the bioreaction. This strategy is applied in this work (in this work, the parameter *vvm* is used instead of F_G, because it is commonly used. *vvm* is defined as $(vvm = F_G/V_L)$, where V_L is the bioreactor working volume. *vvm* is expressed in the units of minutes^{-1}).

A numerical method approach was applied, whereby the bioreaction kinetics and oxygen transfer modelling were used to simulate the bioreaction. In particular, it was applied to calculate C_{OL} at each time step during the bioreaction, as illustrated in Figure 1, and to evaluate the agitator and compressor

electrical power/energy requirements. A PID control algorithm was applied to vary the value of *vvm* (and *Pag*) throughout the fermentation to maintain C_{OL} around a constant specified value (this is referred to as **strategy C**). The time step used in the numerical method approach was 10^{-4} h or 0.36 s. The computations were implemented in Matlab (MathWorks, Natick, MA, USA).

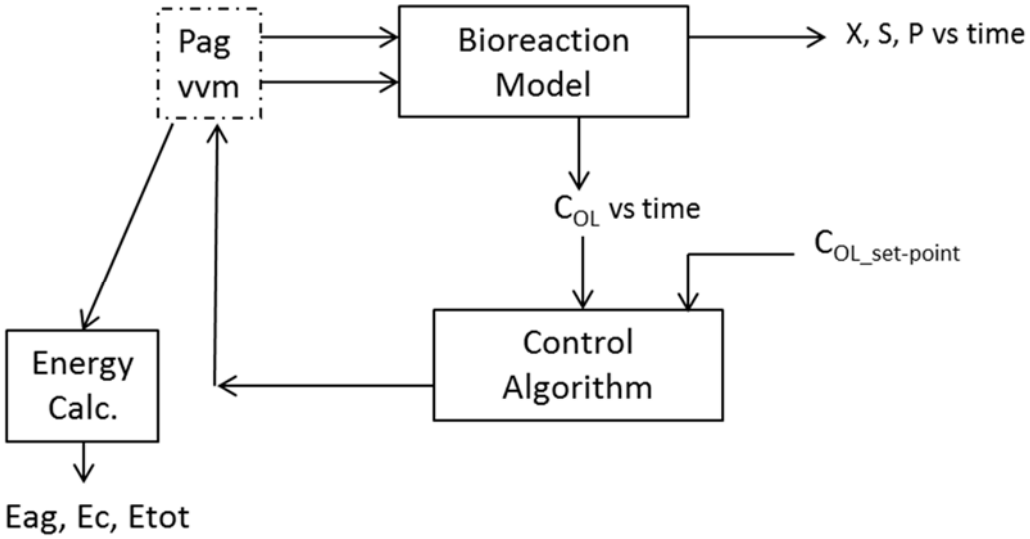

Figure 1. General schematic of control strategy.

There are a number of sub-strategies within strategy C which were investigated. Initially, *Pag* was kept constant and *vvm* was varied throughout the fermentation (this is referred to as **strategy C1**). Subsequently, from an oxygen transfer energy perspective, it is shown that dividing the bioreaction time up into two or more time segments with different constant *Pag* values, where *vvm* is varied in each time segment, might result in major energy savings (this is referred to as **strategy C1-N**, where *N* is the number of time segments).

Further, it is shown that there is a *Pag-vvm* combination profile over time that minimises the total electrical energy that is required for strategy C. This is referred to as **strategy Cmin**. It is shown that the optimal *Pag-vvm* combinations often occur at the onset of the flooding constraint. Consequently, from a control perspective, it is important to able to detect the onset of flooding from the C_{OL} data only. This is integrated into the C1-N control strategy, in particular, and it is referred to as **strategy $C1_F$-N**.

3. Results and Discussion

3.1. Bioreaction Progression

Figure 2a presents the evolution of sugar, product and cell concentrations, and *OUR* over the duration of the bioreaction. The bioreaction time is about 26.5 h when the oxygen concentration in the bioreaction liquid is maintained at 2 mg L^{-1}. The bioreaction progresses slowly over the first 10 h, after which there are significant changes in the concentrations, and the *OUR* reaches a maximum of 4.7 g L^{-1} h^{-1} towards the end of the bioreaction. Figure 2b shows the influence of oxygen concentration in the bioreaction liquid on the specific growth rate. There is a progressive decrease in specific growth rate as the oxygen concentration is reduced below about 2 mg L^{-1}.

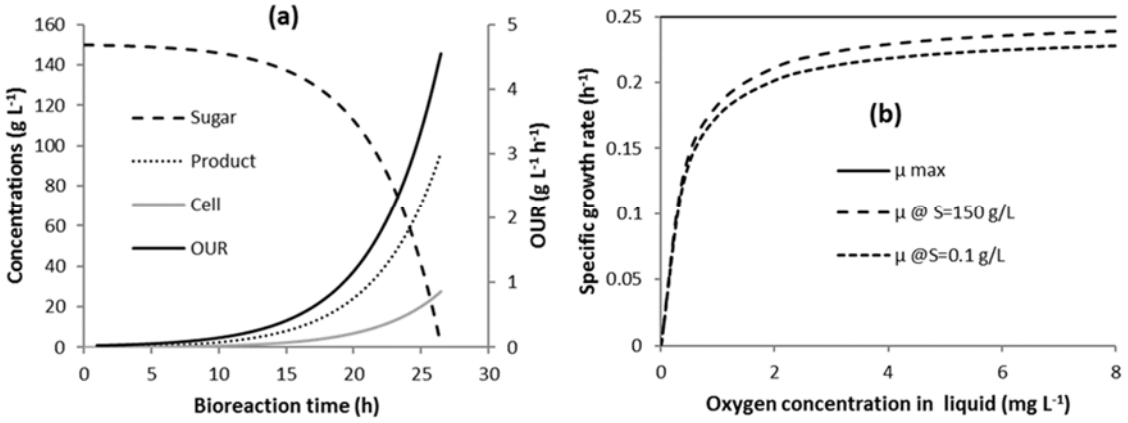

Figure 2. Bioreaction kinetics: (**a**) Cell, sugar, and product concentrations and oxygen uptake rate (OUR) (Strategy C1: C_{OL} = 2 mg L^{-1}, *Pag* = 38.5 kW); and, (**b**) effect of oxygen concentration and sugar concentration (S) on specific growth rate.

3.2. Control of vvm in Strategy C1

For control strategy C1, *Pag* is assigned a constant value, such that flooding does not occur throughout the bioreaction. The lowest value of *Pag* for the bioreaction without flooding is approximately 38.5 kW. A PID control algorithm was developed to continuously vary *vvm* over time, so as to maintain C_{OL} close to 2 mg L^{-1}. The PID controller continuously evaluates an error value $e(t)$ as the difference between a desired set point (C_{OL} = 2 mg L^{-1}) and the value of C_{OL} evaluated from the model. It then calculates a value of the control variable $vvm(t)$ to minimise the error $e(t)$. The new value of $vvm(t)$ is based on the sum of proportional, integral, and derivative (PID) terms in Equation (1):

$$vvm(t) = K_p e(t) + K_i \int_0^t e(t)dt + K_d \frac{de(t)}{dt} \quad (1)$$

The constants K_p, K_i and K_d, were determined using the Ziegler-Nichols tuning method [31]. This is composed of the following steps:

(1) Set a low K_p value (1 or 10 for example) and set $K_i = K_d = 0$.
(2) While $K_i = K_d = 0$, increase K_p value until C_{OL} sustained oscillations appear. The K_p value where oscillations appear is called K_{p_lim}.
(3) Measure oscillation period T_0.
(4) Tune PID parameters using Equations (2) to (4).

$$K_p = 0.6\, K_{p\_lim} \quad (2)$$

$$\tau_i = 0.5\, T_0 \quad (3)$$

$$\tau_d = 0.125\, T_0 \quad (4)$$

where $\tau_i = K_p/K_i$ and $\tau_d = K_d/K_p$.

K_{p_lim} and T_0 were evaluated as 16 and 0.002 h, respectively, and the PID parameters were evaluated from Equations (2) to (4) as K_p = 9.6; τ_i= 0.001 h; τ_d= 0.00025 h, from which K_i and K_d were evaluated.

The control algorithm worked very well for the simulated bioreaction, After the initial part of the bioreaction, where the C_{OL} is allowed decrease from 8 to 2 mg L^{-1}, the variation of C_{OL} throughout the bioreaction was very small in the range of 2 ± 0.03 mg L^{-1}.

The duration of the time step in the simulation is 10^{-4} h or 0.36 s, thus the compressor air flowrate is being changed in the simulation at the end of each time step. This is a short period of time, thus the impact of compressor change time (Δt_C) or time interval between changing the compressor air flowrate

was investigated. The simulations were performed with values of Δt_C greater than 0.36 s. It was found that the PID controller worked well up to about Δt_C = 5 s, but oscillations started to appear in the first half of the bioreaction at higher values of Δt_C.

3.3. Energy Reduction and Minimisation

3.3.1. Energy Minimisation Using Strategy Cmin

OUR varies throughout the bioreaction time during batch operation, as illustrated in Figure 2a. At a specific time during the bioreaction, many different combinations of *vvm* and *Pag* can be determined in order to provide an *OTR* that satisfies the *OUR* at that time in order to maintain a constant C_{OL} value, subject to the constraints. Each of these combinations will have different power requirements. Consequently, for a specific value of *OUR*, there exists an optimum combination of *Pag* and *vvm* that minimises the oxygen transfer total power requirement, subject to constraints [29].

The simulations were performed (at a constant C_{OL} of 2 mg L^{-1}) during the bioreaction time to determine the combinations of *vvm* and *Pag* that minimise the total power requirement at each time increment during the bioreaction. Consequently, the minimum total energy requirement for the bioreactor is achieved by continuously controlling the bioreactor at these optimal combinations of *Pag* and *vvm* throughout the entire bioreaction, and this is referred to as strategy Cmin. This was simulated and Table 1 presents the electrical energy requirements for Cmin, along with the C1 energies for comparison. For the Cmin simulation, the minimum total power requirements throughout the bioreaction occurred at the onset of flooding.

Table 1. Comparison of energy requirements (MJ) for the different strategies (set-point C_{OL} = 2 mg L^{-1}). The % energy savings are relative to strategy C1.

Control Strategy	Agitator *Eag*	Compressor *Ec*	Total E_{tot}	Energy Savings (%)
C1	4104	459	4563	-
Cmin	746	706	1452	68.2
C1-2	2174	463	2637	42.2
C1-5	1221	529	1750	61.6
C1-10	965	590	1555	65.9

The power requirements will depend on the values of *OUR*, the k_La correlation, and the constraints. Fitzpatrick et al. [29] performed simulations for a typical range of OUR values, bioreactor working volumes, and for five k_La correlation equations. These simulations applied the same bioreaction kinetics as in this work. These simulations showed that the minimum total power requirement tended to be constrained by flooding for many of the scenarios, and it was close to the flooding value for those where the minimum was obtained before the occurrence of flooding. Overall, the simulations suggest that the scenario C minimum total energy can be achieved by the controlling *vvm*–Pag combinations at the onset of flooding throughout the bioreaction.

3.3.2. Energy Reduction Using Strategy C1-N

Scenario Cmin might not be practical, because it involves trying to continuously control *vvm* and *Pag*, so that they are at the onset of flooding throughout the bioreaction. In strategy C1, *Pag* is kept constant and *vvm* was varied throughout the fermentation. *Pag* has a lower limiting value, whereby if *Pag* is chosen below this limiting value, then the *vvm* required at maximum *OUR* exceeds the flooding *vvm* and C_{OL} cannot be maintained constant. Operating at this limiting value of *Pag* throughout the bioreaction time results in relatively high total energy requirement due to the high agitator energy requirement.

Fitzpatrick et al. [29] suggests that this energy requirement can be greatly reduced by applying strategy C1-N, where the bioreaction time is divided up into *N* time segments (two or more time

segments), where lower constant *Pag* values are applied in each time segment without flooding the impeller. For the model bioreaction, the *OUR* progressively increases with time with the maximum being near the end, as illustrated in Figure 2a. This bioreaction could be divided up into *N* time segments with *Pag* progressively increasing from segment to segment, up until the limiting *Pag* value in strategy C1 in the last time segment.

Figure 3 illustrates the variation in *Pag*, *vvm* and C_{OL} for a five-segment control strategy (C1-5) where the time duration of each segment is equal. Figure 3a shows the values of *Pag* in each time segment. Within each time segment, the value of *Pag* represents the lowest value without the occurrence of impeller flooding. The non-linear increase in *Pag* from segment to segment is due to *OUR* increasing non-linearly, as illustrated in Figure 2a. Figure 3b shows how *vvm* is varied by the control algorithm. Within each time segment, *vvm* increases, as expected, and then decreases when there is a transition from one segment to the next with the step increase in *Pag*. This step increase in *Pag* causes significant variation in C_{OL}, as illustrated in Figure 3b; however, this is only for a short duration after the transition. Otherwise, the control algorithm works very well in controlling C_{OL}. In fact, the variation at the transition can be greatly reduced by introducing a more gradual increase in *Pag* at the end of each time segment, rather than a step increase.

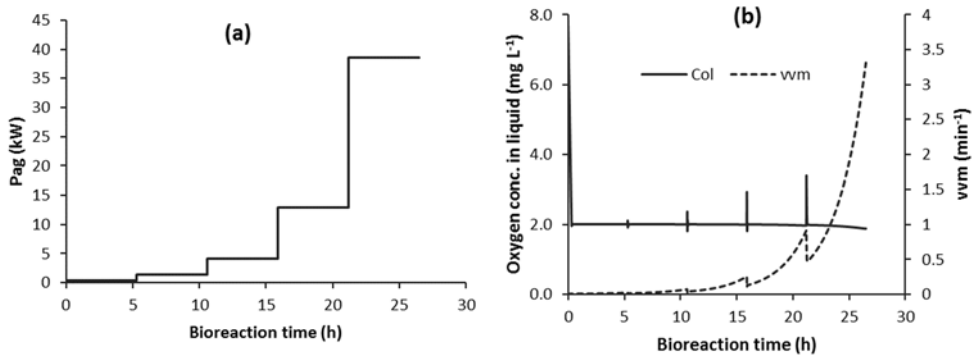

Figure 3. Scenario C1-5: Effect of proportional, integral, and derivative (PID) control on (**a**) *Pag* step increases and (**b**) C_{OL} and vvm (five equal time segments—non-flooding).

Simulations were performed to compare the energy requirements of strategies C1-N with C1 and Cmin, and Table 1 presents the results. Increasing the number of time segments results in a major reduction in the total energy requirement for oxygen transfer. Dividing the bioreaction time into two time-segments results in a 42% energy reduction. Dividing the bioreaction time into 10 time-segments results in a 66% energy reduction. Consequently, there is a diminishing additional energy saving that is associated with each additional time segment. Increasing the number of time segments will progressively approach that of Cmin.

3.4. Implementation of Strategy C1-N with Detection of Impeller Flooding using Oxygen Sensor Data ($C1_F$-N)

Section 3.3 suggests that energy can be minimised by operating at or close to the onset of impeller flooding throughout the duration of the bioreaction; however, this might not be operable from a practical control perspective. Strategy C1-N, using a small number of time segments, is practically operable, and Section 3.3 suggests that this could obtain most of the energy savings that are associated with Cmin. For example, the data provided in Table 1 show that operating with 10 equal time segments (C1–10) provides 96.6% of the savings made by Cmin relative to strategy C1.

The problem with strategy C1-N, as outlined in Section 3.3, is that it inherently assumes that the relationship between the flooding *vvm* and *Pag* is known. Such correlations do exist [32], however these are only approximations. Consequently, it would advantageous if the controller could detect the onset of flooding while using the measured C_{OL} data. With this, the controller could implement a step increase in *Pag* once it detected flooding and automatically moved to the next time segment.

3.4.1. Detection of Impeller Flooding Using Oxygen Sensor Data and Implementation of Strategy $C1_F$-N

Considering the above, work was undertaken to develop an algorithm that could detect the onset of flooding. Before doing this, a k_La model for the flooding region had to be developed, so that k_La in the simulated bioreaction would decrease in the flooded region. As a first attempt, a simplified model for estimating k_La in the flooded region was constructed. This essentially consisted of applying the k_La correlation Equation (5), such that it is symmetrical around the flooding air superficial velocity (v_{sF}), as presented in Equation (6), where air superficial velocity (v_s) is defined as air volumetric flowrate per unit cross-sectional area of bioreactor [29]. Figure 4 illustrates how *vvm* and *Pag* influence k_La in the non-flooded and flooded regions for two values of *Pag*.

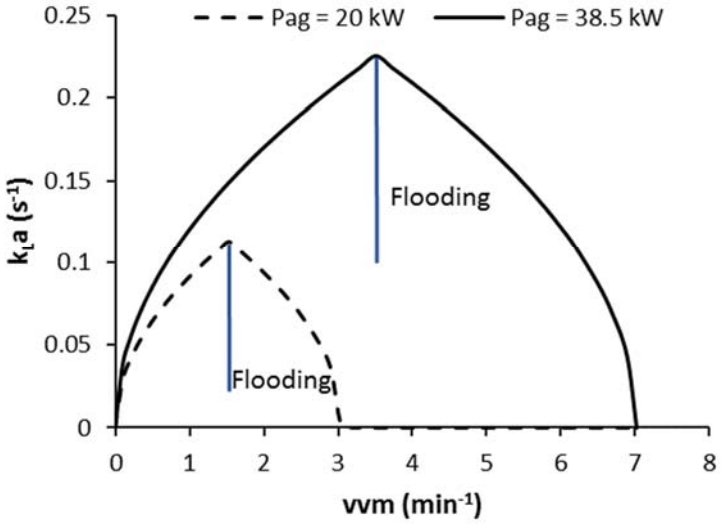

Figure 4. Effect of *vvm* and *Pag* on k_La in the non-flooded and flooded regions using a symmetrical k_La model.

Region 1:

$$v_s \leq v_{sF}$$
$$k_La = K\left(\frac{Pag}{V_L}\right)^{n1}(v_s)^{n2} \quad (5)$$

Region 2:

$$v_{sF} < v_s \geq 2\, v_{sF}$$
$$k_La = K\left(\frac{Pag}{V_L}\right)^{n1}(v_{sF} - (v_s - v_{sF})^{n2} \quad (6)$$

Region 3:

$$v_s > 2\, v_{sF}$$
$$k_La = 0$$

The work on developing a flooding detection algorithm first looked at how the model behaved when the simulated flooding occurred. This is presented in Figure 5 for a strategy C1 case where flooding occurs during the bioreaction. *Pag* was assigned a constant value of 3.8 kW, which is well below the value of *Pag* where the onset of flooding occurs at the maximum *OUR* for the non-flooded case (~38.5 kW). The flooding occurred at about 15.51 h into the bioreaction, as can be seen in Figure 5 by the rapid decrease in C_{OL}, which took approximately 45 s to decrease from the set-point of 2 mg L^{-1} down to 0. This is because as C_{OL} decreases due to the increase in *OUR*, the controller responds by increasing *vvm* to increase the *OTR*. However, this is counterproductive once *vvm* is in the flooded region and it causes k_La (and *OTR*) to decrease rather than increase, which, in turn, causes C_{OL} to decrease rapidly. This rapid continuous decrease in C_{OL} was used to detect the onset of flooding. Flooding was detected when C_{OL} decreased below a certain value (referred to as C_{OL_FLD}), which was

below the 2 mg L^{-1} control set-point. Simulations were first performed at a value of C_{OL_FLD} that was equal to 1.9 mg L^{-1} and this worked well. However, significant fluctuations in C_{OL} occur after the subsequent increase in *Pag*, thus flooding detection had to be suspended for a short time period after the *Pag* transition.

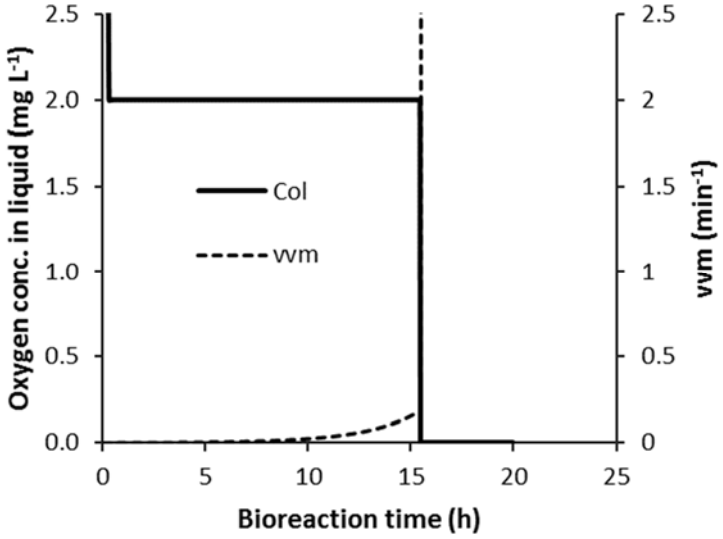

Figure 5. Effect of flooding on control strategy C1. (*Pag* = 3.8 kW and flooding occurs at 15.51 h).

The flooding detection was then integrated into the C1-N control strategy and it is referred to as strategy $C1_F$-N. To implement the $C1_F$-N strategy, it is first necessary to estimate a high enough value of *Pag* (Pag_{max}), such that flooding does not occur at maximum *OUR*. This is, in essence, sizing the mechanical power requirement of the agitator. One approach to doing this is to experimentally measure the maximum *OUR* at a small scale for the bioreaction. Subsequently, the modelling equations that were presented by Fitzpatrick et al. [29], including a relevant k_La correlation, were be applied to gain an estimate of *Pag* at the onset of flooding for the maximum *OUR* value, as was carried out for Figure 3. This can also be used to provide an estimate on the maximum *vvm* requirement (vvm_{max}), which essentially sizes the air compressor and prevents any excessive airflow response by the PID controller.

Once Pag_{max} is estimated, the $C1_F$-N control strategy is implemented, as follows:

A step increase in *Pag* from time segment to time segment (ΔPag) is defined in Equation (7).

$$\Delta Pag = \frac{Pag_{max}}{N} \tag{7}$$

Subsequently, the *Pag* in each time segment (Pag_i) (where *i* is an integer starting at 1) is given in Equation (8).

$$Pag_i = i \times \Delta Pag \tag{8}$$

This is a little different to the previous implementation of C1-N where the time segments were of equal duration, but the step increases in *Pag* varied in magnitude, as illustrated in Figure 3. Currently, the durations are different, but the step increases in *Pag* are the same. This is illustrated in Figure 6 for five time segments ($C1_F$-5). This is more practical, because it is not known exactly what the flooding *Pag* is at the end of each time segment for the case of using equal time segment durations.

Further simulations were performed for two and 10 segments and Table 2 presents the energy requirements, and these can be compared with C1-N presented in Table 1, where there was no flooding detection. The energy requirements and energy savings are similar, but they are a little greater for the cases while using flood detection. This is most likely because the segment time durations and *Pag* values in each time segment are different.

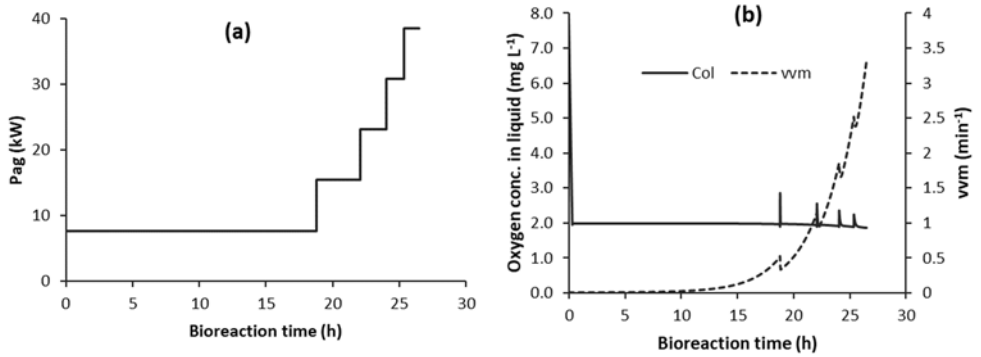

Figure 6. Control strategy $C1_F$-5 (with automatic detection of flooding; C_{OL_FLD} = 1.9 mg L^{-1}): (**a**) Pag step increases; and, (**b**) C_{OL} and *vvm*.

Table 2. Comparison of energy requirements (MJ) for the strategies with onset of flooding detection ($C1_F$-N) (set-point C_{OL} = 2 mg L^{-1}). The % energy savings are relative to strategy C1.

Control Strategy	Agitator *Eag*	Compressor *Ec*	Total E_{tot}	Energy Savings (%)
C1	4104	459	4563	-
Cmin	746	706	1452	68.2
Strategy $C1_F$-N				
$C1_F$-2	2303	520	2823	38.1
$C1_F$-5	1305	596	1901	58.3
$C1_F$-10	1001	635	1637	64.1

In the results shown above, the simulations were performed at C_{OL_FLD} = 1.9 mg L^{-1}, which is only 0.1 mg L^{-1} below the control set-point of 2 mg L^{-1}. The PID controller performed well in controlling C_{OL} in the simulated bioreactions; however, random fluctuations in real oxygen sensor measurements could cause the measured C_{OL} to be below 1.9 mg L^{-1} and cause unwanted step increases in *Pag* and greatly reduce the energy saving potential. Consequently, the influence of random fluctuations in the oxygen sensor measurements are investigated in the next section.

3.4.2. Dealing with Random Fluctuations in the Oxygen Sensor Measurements and Unwanted Pag Step Increases

Random fluctuations in real oxygen sensor measurements could cause unwanted step increases in *Pag*, which would greatly reduce the energy saving potential. This is highly undesirable. A number of factors could cause the random fluctuations, including the medium being two-phase consisting of air bubbles in aqueous liquid and variations in oxygen concentrations due to non-ideal mixing. This section examines the impact of these fluctuations and how they can be overcome. The impact of random fluctuations is included in the modelling through Equation (9).

$$C_{OL\_sensor} = C_{OL}\,(1 + x\,Y) \tag{9}$$

where C_{OL_sensor} is the simulated oxygen sensor measurement, Y is the maximum fluctuation amplitude (mg L^{-1}), and x is a random number generated between −1 and +1. The error value $e(t)$ is now calculated as the difference between a desired set point (C_{OL} = 2 mg L^{-1}) and the value of C_{OL_sensor}, and this is used in the PID controller equation (1) in order to evaluate *vvm*.

This was initially applied for Y = 0.2 and C_{OL_FLD} = 1.9 mg L^{-1}. Figure 7a shows the random fluctuation in sensor oxygen concentration in the liquid (C_{OL_sensor}), and Figure 7b shows its effect on *Pag*. When compared to Figure 6a, this shows the *Pag* step increases occurring much earlier than desired and, consequently, the energy saving potential is lost. This simply occurs because the random

fluctuations (with $Y = 0.2$) causes C_{OL_sensor} to randomly decrease below C_{OL_FLD} activating unwanted step increases in *Pag*. This causes a fluctuation in *vvm*, which causes the real value of the oxygen concentration in the liquid (C_{OL}) to also vary, as illustrated in Figure 7c.

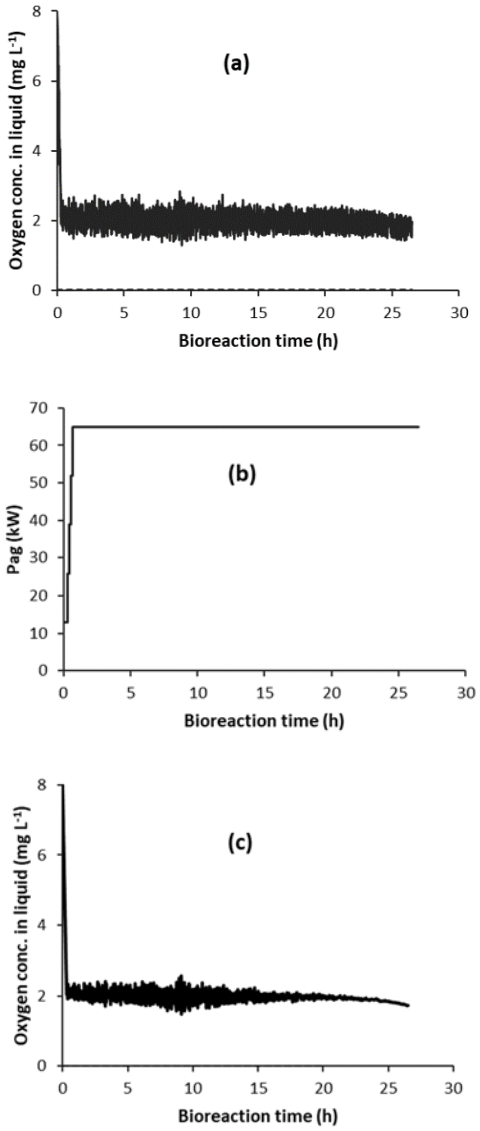

Figure 7. (**a**) Random fluctuation ($Y = 0.2$) of sensor oxygen concentration in liquid (C_{OL_sensor}), and its effect on the evolution of (**b**) *Pag*, and (**c**) C_{OL} for control strategy $C1_F$-5 (with automatic detection of flooding; $C_{OL\_FLD} = 1.9$ mg L^{-1}).

One approach for trying to prevent the random fluctuations causing unwanted *Pag* step increases is to reduce the value of C_{OL_FLD}. From Equation (9) and considering that C_{OL} is fluctuating around its set-point (C_{OL_sp}), then unwanted *Pag* step increases will occur if the condition in Equation (10) is met.

$$C_{OL\_sp}(1 - Y) < C_{OL\_FLD} \tag{10}$$

When considering this, simulations were run for combinations of Y (= 0.1, 0.3, 0.5) and C_{OL_FLD} (= 1.9, 1.7, 1.5, 1.2, 0.8) to evaluate whether unwanted *Pag* step increases occurred or not, and Table 3 presents the results. The results show that an unwanted *Pag* step increase did occur when the condition in Equation (10) was met. Furthermore, Table 3 shows some unwanted *Pag* step increases occurring for some C_{OL_FLD} lower than in the condition, and this is due to the random fluctuation in the C_{OL} value below the set-point value (Figure 7c).

Table 3. Effect of Y and C_{OL_FLD} on whether or not unwanted *Pag* step increases occurred (Yes/No) (set-point C_{OL} = 2 mg L^{-1}).

C_{OL_FLD} (mg L^{-1})	Y = 0.1	Y = 0.3	Y = 0.5
0.8	No	No	Yes
1.2	No	Yes	Yes
1.5	No	Yes	Yes
1.7	Yes	Yes	Yes
1.9	Yes	Yes	Yes

Colour signifies that constraint in Equation (10) was met.

Reducing the effect of the fluctuations by applying a moving average to fluctuation in C_{OL_sensor} (i.e., C_{OL_senMA}) is another approach for trying to prevent the random fluctuations causing unwanted *Pag* step increases. This was implemented in the model by evaluating the average of C_{OL_sensor} over the last ten time steps. Figure 8 illustrates the effect of using moving average to reduce the fluctuations. This had a beneficial impact on reducing unwanted step increases in *Pag*, as the first "Yes" in Table 3 became a "No" for each of the values of Y. Care has to be taken not to have too long a time duration over which a moving average is calculated as it introduces a time delay.

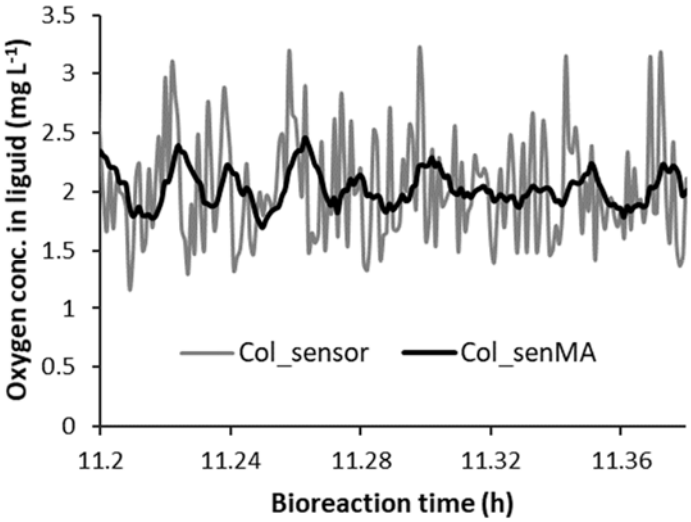

Figure 8. Comparison of the sensor oxygen concentration in liquid (C_{OL_sensor}) and its moving average (C_{OL_senMA}).

3.4.3. Impact of Operating at Lower Values of C_{OL_FLD}

To avoid the effect of random fluctuations in the oxygen sensor measurements (C_{OL_sensor}) causing unwanted *Pag* step increases, it may be necessary to operate at lower values of C_{OL_FLD}, as outlined in the previous section. Some of the $C1_F$-5 simulations that were run at lower values of C_{OL_FLD} (typically below 0.8 mg L^{-1}) showed an unusual behaviour. This occurred in simulations both with and without random fluctuations, thus the root cause of this behaviour was not the presence of the random fluctuations. Figure 9 illustrates the behaviour, where there was a lower number of *Pag* step increases (one less in Figure 9a) and an unusual C_{OL} profile towards the end of the bioreaction (Figure 9b). This behaviour did not have a major influence on bioreaction time or total energy requirement, even at a very low C_{OL_FLD} of 0.1 mg L^{-1}, where the bioreaction time increased by 0.2 h and the total energy increased by 3.7%.

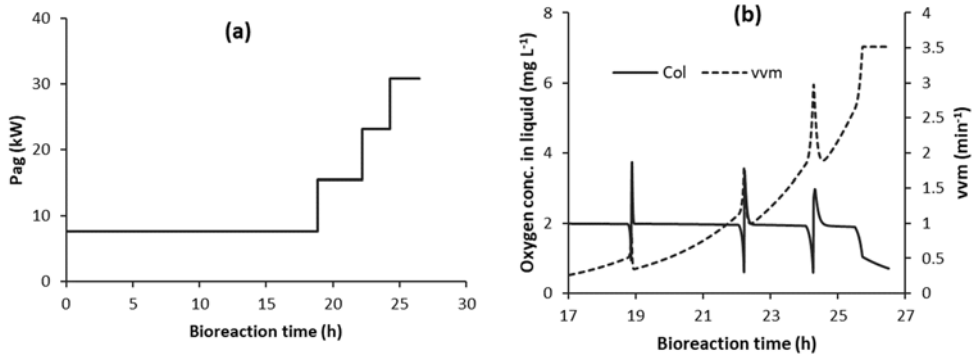

Figure 9. Effect of C_{OL_FLD} = 0.5 mg L^{-1} on control strategy $C1_F$-5 (with automatic detection of flooding; $Y = 0$): (**a**) Pag step increases; and, (**b**) C_{OL} and vvm (Note: time starts at 17 h).

The rationale for the behaviour is somewhat complex. Before a *Pag* step increase, C_{OL} decreases towards C_{OL_FLD} due to the onset of flooding and the PID controller correspondingly causes an increase in *vvm*, as illustrated in Figure 9b. This moves the system further into the flooding zone, which reduces k_La and causes C_{OL} to rapidly decrease. This usually results in a *Pag* step increase when C_{OL} decreases to C_{OL_FLD}. However, in the latter part of the bioreaction (Figure 9b), the rate of decrease of C_{OL} suddenly changed to a slower rate and C_{OL} decreased more slowly towards C_{OL_FLD}. This sudden transition corresponded to, or was triggered by, *vvm* attaining its maximum value (vvm_{max}). This is a specified value in the model that equals the value of *vvm* at the onset of flooding at the final value of *Pag*. Once *vvm* becomes constant, k_La also attains a constant value, and a complex interplay between variables occurs, which causes C_{OL} to decrease at a much slower rate. This slower decrease in C_{OL} results in C_{OL} not being reduced to C_{OL_FLD} before the end of the bioreaction (as illustrated in Figure 9b) and, thus, the final *Pag* step was not triggered (Figure 9a).

An initial suggestion to overcome this might be to increase the value of vvm_{max}, because limiting this value caused the slowing of the decreases in C_{OL} that resulted in the final *Pag* step increase not being triggered. This was simulated; however, the modelling showed that this worked for some simulations, but not so for other simulations, especially those at low values of C_{OL_FLD}. The reason for this approach not working is because increasing *vvm* beyond the original specified vvm_{max} does trigger the *Pag* step increase as desired; however, the higher *vvm* is in the flooding zone at the higher final *Pag* value. How far it is into the flooding zone has a major influence on k_La and *OTR*. If too far into the flooding zone, insufficient *OTR* is developed and C_{OL} will continue to decrease towards zero, slowing the bioreaction and significantly increasing the bioreaction time.

The net effect of the above is that reducing C_{OL_FLD} to low values, e.g., <0.8 mg L^{-1} in the simulations, can result in complex dynamics occurring, as highlighted above. However, it might not be necessary to operate at such low values of C_{OL_FLD} and, consequently, the issue will not manifest itself. Furthermore, the behaviour that is illustrated in Figure 9 resulted in a minor reduction in bioreactor performance, with only small increases in energy requirement and bioreaction time.

4. Conclusions

A PID controller was used to control *vvm*, so as to maintain C_{OL} at a constant value of 2 mg L^{-1} throughout a simulated bioreaction whose *OUR* progressively increased over time. When *Pag* is kept constant throughout the bioreaction, this leads to excessive oxygen transfer energy requirement, because a high value of *Pag* is required at maximum *OUR* to prevent flooding. Operating at or near the impeller flooding constraint throughout the bioreaction results in the minimum energy requirement for oxygen transfer (strategy Cmin); however, this might prove impractical to control and operate in practice. It was shown that most of the energy saving that is associated with Cmin could be achieved by dividing the bioreaction time into a small number of time segments (e.g., 5) with lower constant *Pag* values. The onset of flooding occurs at the end of each time segment and this initiates a *Pag* step

increase for the next time segment. To implement this, the onset of flooding needs to be detected in order to signal the increase in *Pag*. This was achieved while using the simulated C_{OL} vs. time data, where there was a rapid decrease in C_{OL} when flooding occurred, and this was used to detect the onset of flooding and initiate the step increase in *Pag* for the next time segment. Random fluctuations in the oxygen sensor readings can cause unwanted *Pag* step increases, which could reduce the energy saving potential; however, the incorporation of lower values of C_{OL_FLD} and moving averages can overcome this problem. The insights developed in this paper are coming from mathematical modelling simulations and some practical insights (such as sensor measurement fluctuations); consequently, practical experimental and pilot scale work is required to test and further develop the presented ideas. Furthermore, there might be other practical constraints that may influence the determination of *vvm* and *Pag* and impact on the energy reduction potential, such as foaming and the shear sensitivity of cells. Finally, the control of oxygen transfer coupled with reducing the energy requirement is complex, as there are many variables that can interact with each other, which sometimes might result in unusual non-intuitive behaviours. The implementation of modelling simulations and interrogating the resulting data can help to explain these behaviours.

Author Contributions: J.J.F. supervised all of the work presented in the paper and wrote the paper. F.G., E.M. contributed to the development of the mathematical models, execution of the models to generate the results and to the analysis and interpretation of the results. All authors have read and agreed to the published version of the manuscript.

Funding: This research received no external funding.

Conflicts of Interest: The authors declare no conflict of interest.

List of Symbols

C_{OL}	oxygen concentration in the bioreaction liquid (mg L^{-1})
C_{OL_FLD}	oxygen concentration at which *Pag* step increase occurs (mg L^{-1})
C_{OL_sensor}	simulated oxygen sensor measurement (mg L^{-1})
$_{OL\_senMA}$	moving average of C_{OL_sensor} values (mg L^{-1})
C_{OL_sp}	oxygen concentration controller set-point (mg L^{-1})
Eag	agitator electrical energy (GJ)
Ec	compressor electrical energy (GJ)
E_{tot}	sum of agitator and compressor electrical energy (GJ)
$e(t)$	difference between O_2 concentration set-point and simulated value (mg L^{-1})
F_G	inlet air volumetric flowrate (m^3 h^{-1})
k_La	volumetric oxygen mass transfer coefficient (h^{-1})
K_d K_i K_p	PID controller constants
N	number of time increments
OUR	oxygen uptake rate (g L^{-1} h^{-1})
OTR	oxygen transfer rate (g L^{-1} h^{-1})
P	product concentration (g L^{-1})
Pag	agitator mechanical power input (kW)
S	sugar concentration (g L^{-1})
t	time (hours)
T_0	oscillation period PID controller (h)
V_L	bioreactor working volume (m^{-3})
vvm	volume of air per minute per unit bioreactor working volume (min^{-1})
v_s	air superficial velocity (m h^{-1})
v_{sF}	air superficial velocity at onset of flooding (m h^{-1})
X	cell concentration (g L^{-1})
Y	maximum random fluctuation amplitude in oxygen concentration (mg L^{-1})
μ	specific growth rate (h^{-1})
μ_{max}	maximum specific growth rate (h^{-1})
τ_i τ_d	PID controller parameters (h)

References

1. García-Ochoa, F.; Gomez, E. Bioreactor scale-up and oxygen transfer rate in microbial processes: An overview. *Biotechnol. Adv.* **2009**, *27*, 153–176. [CrossRef] [PubMed]
2. Juarez, P.; Orejas, J. Oxygen transfer in a stirred reactor in laboratory scale. *Lat. Am. Appl. Res.* **2001**, *31*, 433–439.
3. Demirtas, M.U.; Kolhatkar, A.; Kilbane, J.J. Effect of aeration and agitation on growth rate of Thermus thermophilus in batch mode. *J. Biosci. Bioeng.* **2003**, *95*, 113–117. [CrossRef]
4. Bandaiphet, C.; Prasertsan, P. Effect of aeration and agitation rates and scale-up on oxygen transfer coefficient, kLa in exopolysaccharide production from Enterobacter cloacae WD7. *Carbohydr. Polym.* **2006**, *66*, 216–228. [CrossRef]
5. Huang, W.-C.; Chen, S.-J.; Chen, T.-L. The role of dissolved oxygen and function of agitation in hyaluronic acid fermentation. *Biochem. Eng. J.* **2006**, *32*, 239–243. [CrossRef]
6. Emily, L.; Nandong, J.; Samyudia, Y. Experimental Investigation on the Impact of Aeration Rate and Stirrer Speed on Micro-Aerobic Batch Fermentation. *J. Appl. Sci.* **2009**, *9*, 3126–3130. [CrossRef]
7. Radchenkova, N.; Vassilev, S.; Martinov, M.; Kuncheva, M.; Panchev, I.; Vlaev, S.; Kambourova, M. Optimization of the aeration and agitation speed of Aeribacillus palidus 418 exopolysaccharide production and the emulsifying properties of the product. *Process. Biochem.* **2014**, *49*, 576–582. [CrossRef]
8. Tervasmäki, P.; Latva-Kokko, M.; Taskila, S.; Tanskanen, J. Effect of oxygen transfer on yeast growth—Growth kinetic and reactor model to estimate scale-up effects in bioreactors. *Food Bioprod. Process.* **2018**, *111*, 129–140. [CrossRef]
9. Felder, M.; Simmons, A.; Shambaugh, R.; Sikavitsas, V. Effects of Flow Rate on Mesenchymal Stem Cell Oxygen Consumption Rates in 3D Bone-Tissue-Engineered Constructs Cultured in Perfusion Bioreactor Systems. *Fluids* **2020**, *5*, 30. [CrossRef]
10. Alves, S.S.; Vasconcelos, J.M.T. Optimisation of agitation and aeration in fermenters. *Bioprocess Eng.* **1996**, *14*, 119–123. [CrossRef]
11. Humbird, D.; Davis, R.; McMillan, J.D. Aeration costs in stirred-tank and bubble column bioreactors. *Biochem. Eng. J.* **2017**, *127*, 161–166. [CrossRef]
12. Benz, G.T. Impeller selection for agitated aerobic fermenters. *Chem. Eng. Prog.* **2004**, *100*, 18S–20S.
13. Buffo, M.; Corrêa, L.; Esperança, M.; Cruz, A.J.G.; Farinas, C.; Badino, A.C. Influence of dual-impeller type and configuration on oxygen transfer, power consumption, and shear rate in a stirred tank bioreactor. *Biochem. Eng. J.* **2016**, *114*, 130–139. [CrossRef]
14. Schaepe, S.; Kuprijanov, A.; Sieblist, C.; Jenzsch, M.; Simutis, R.; Lübbert, A. kLa of stirred tank bioreactors revisited. *J. Biotechnol.* **2013**, *168*, 576–583. [CrossRef]
15. Gakingo, G.; Clarke, K.; Louw, T. A numerical investigation of the hydrodynamics and mass transfer in a three-phase gas-liquid-liquid stirred tank reactor. *Biochem. Eng. J.* **2020**, *157*, 107522. [CrossRef]
16. Rahimi, M.J.; Sitaraman, H.; Humbird, D.; Stickel, J.J. Computational fluid dynamics study of full-scale aerobic bioreactors: Evaluation of gas–liquid mass transfer, oxygen uptake, and dynamic oxygen distribution. *Chem. Eng. Res. Des.* **2018**, *139*, 283–295. [CrossRef]
17. De Jesus, S.S.; Neto, J.M.; Filho, R. Hydrodynamics and mass transfer in bubble column, conventional airlift, stirred airlift and stirred tank bioreactors, using viscous fluid: A comparative study. *Biochem. Eng. J.* **2017**, *118*, 70–81. [CrossRef]
18. Nienow, A.W. Mass transfer and mixing across the scales in animal cell culture. In *Animal Cell Culture*; Al-Rubeai, M., Ed.; ; Volume 9, Cell Engineering; Springer: Cham, Switzerland, 2015.
19. Benz, G.T. Optimize power consumption in aerobic fermenters. *Chem. Eng. Prog.* **2003**, *99*, 32–35.
20. Benz, G.T. Cut agitator power costs. *Chem. Eng. Prog.* **2012**, *108*, 40–43.
21. Zamouche, R.; Bencheikh-Lehocine, M.; Meniai, A.-H. Oxygen transfer and energy savings in a pilot-scale batch reactor for domestic wastewater treatment. *Desalination* **2007**, *206*, 414–423. [CrossRef]
22. Hu, D.; Luo, K.; Ma, H.; Min, H.; Zhao, Y.; Cui, Y.; Wang, S.; Ning, N.; Zhang, L.; Liu, W. A sustainability anti-infective pharmaceutical wastewater treatment technology: Multi-stage vertical variable diameter membrane bioreactor with DO online controlling. *Bioresour. Technol.* **2020**, *311*, 123507. [CrossRef] [PubMed]
23. Chitra, M.; Natarajan, P.; Abraham, A. Dissolved Oxygen Control of Batch Bioreactor using Model Reference Adaptive Control scheme. *IFAC-PapersOnLine* **2018**, *51*, 13–18. [CrossRef]

24. Du, X.; Wang, J.; Jegatheesan, V.; Shi, G. Dissolved Oxygen Control in Activated Sludge Process Using a Neural Network-Based Adaptive PID Algorithm. *Appl. Sci.* **2018**, *8*, 261. [CrossRef]
25. Simutis, R.; Lübbert, A. Bioreactor control improves bioprocess performance. *Biotechnol. J.* **2015**, *10*, 1115–1130. [CrossRef]
26. Jonelis, K.; Brazauskas, K.; Levisauskas, D. A system for dissolved oxygen control in industrial aeration tank. *Inf. Technol. Control* **2012**, *41*, 46–52. [CrossRef]
27. Oliveira, R.; Simutis, R.; De Azevedo, S.F. Design of a stable adaptive controller for driving aerobic fermentation processes near maximum oxygen transfer capacity. *J. Process. Control* **2004**, *14*, 617–626. [CrossRef]
28. Kreyenschulte, D.; Emde, F.; Regestein, L.; Büchs, J. Computational minimization of the specific energy demand of large-scale aerobic fermentation processes based on small-scale data. *Chem. Eng. Sci.* **2016**, *153*, 270–283. [CrossRef]
29. Fitzpatrick, J.; Gloanec, F.; Michel, E.; Blondy, J.; Lauzeral, A. Application of Mathematical Modelling to Reducing and Minimising Energy Requirement for Oxygen Transfer in Batch Stirred Tank Bioreactors. *ChemEngineering* **2019**, *3*, 14. [CrossRef]
30. Buffo, M.M.; Esperança, M.N.; Béttega, R.; Farinas, C.S.; Badino, A.C. Oxygen Transfer and Fragmentation of Aspergillus niger Pellets in Stirred Tank and Concentric-Duct Airlift Bioreactors. *Ind. Biotechnol.* **2020**, *16*, 67–74. [CrossRef]
31. Seborg, D.E.; Edgar, T.F.; Mellichamp, D.A.; Doyle, F.J., III. *Process Control and Dynamics*; John Wiley & Sons: Hoboken, NJ, USA, 2011.
32. Bakker, A.; Smith, J.M.; Meyers, K.J. How to disperse gases in liquids. *Chem. Eng.* **1994**, *12*, 98–104.